# Report Documentation Page

*Form Approved*
*OMB No. 0704-0188*



| | | |
|---|---|---|
| 1. REPORT DATE<br>**APR 2006** | 2. REPORT TYPE | 3. DATES COVERED<br>**00-00-2006 to 00-00-2006** |

| | |
|---|---|
| 4. TITLE AND SUBTITLE<br>**W-structured type-II superlattice long-wave infrared photodiodes with high quantum efficiency** | 5a. CONTRACT NUMBER |
| | 5b. GRANT NUMBER |
| | 5c. PROGRAM ELEMENT NUMBER |
| 6. AUTHOR(S) | 5d. PROJECT NUMBER |
| | 5e. TASK NUMBER |
| | 5f. WORK UNIT NUMBER |
| 7. PERFORMING ORGANIZATION NAME(S) AND ADDRESS(ES)<br>**Naval Research Laboratory,4555 Overlook Avenue SW,Washington,DC,20375** | 8. PERFORMING ORGANIZATION REPORT NUMBER |
| 9. SPONSORING/MONITORING AGENCY NAME(S) AND ADDRESS(ES) | 10. SPONSOR/MONITOR’S ACRONYM(S) |
| | 11. SPONSOR/MONITOR’S REPORT NUMBER(S) |

12. DISTRIBUTION/AVAILABILITY STATEMENT
**Approved for public release; distribution unlimited**

13. SUPPLEMENTARY NOTES

14. ABSTRACT

15. SUBJECT TERMS

| 16. SECURITY CLASSIFICATION OF: | | | 17. LIMITATION OF ABSTRACT | 18. NUMBER OF PAGES | 19a. NAME OF RESPONSIBLE PERSON |
|---|---|---|---|---|---|
| a. REPORT<br>**unclassified** | b. ABSTRACT<br>**unclassified** | c. THIS PAGE<br>**unclassified** | **Same as Report (SAR)** | **3** | |

**Standard Form 298 (Rev. 8-98)**
Prescribed by ANSI Std Z39-18

# W-structured type-II superlattice long-wave infrared photodiodes with high quantum efficiency

E. H. Aifer,[a] J. G. Tischler, J. H. Warner, I. Vurgaftman, W. W. Bewley, J. R. Meyer, J. C. Kim, and L. J. Whitman
*Naval Research Laboratory, Washington, DC 20375*

C. L. Canedy and E. M. Jackson
*SFA Inc., Crofton, Maryland 21114*

(Received 18 April 2006; accepted 21 June 2006; published online 4 August 2006)

Results are presented for an enhanced type-II W-structured superlattice (WSL) photodiode with an 11.3 μm cutoff and 34% external quantum efficiency (at 8.6 μm) operating at 80 K. The new WSL design employs quaternary $Al_{0.4}Ga_{0.49}In_{0.11}Sb$ barrier layers to improve collection efficiency by increasing minority-carrier mobility. By fitting the quantum efficiencies of a series of *p-i-n* WSL photodiodes with background-doped *i*-region thicknesses varying from 1 to 4 μm, the authors determine that the minority-carrier electron diffusion length is 3.5 μm. The structures were grown on semitransparent *n*-GaSb substrates that contributed a 35%–55% gain in quantum efficiency from multiple internal reflections. © *2006 American Institute of Physics*. [DOI: 10.1063/1.2335509]

W-structured type-II superlattices (WSLs), which were initially developed to increase the gain in midwave infrared (MWIR) lasers,[1,2] are now showing promise as long-wave and very-long-wave infrared (LWIR and VLWIR) photodiode materials. The WSL addresses the reduced overlap between the wave functions for conduction and valence states in type-II superlattices, arising from the alternating electron and hole confinement layers. In the WSL illustrated in Fig. 1, two InAs "electron wells" are located on either side of an InGaSb hole well and are bound on either side by AlSb (dashed) or AlGaInSb (solid) "barrier" layers. The barriers confine the electron wave functions symmetrically about the hole well, increasing the electron-hole overlap while nearly localizing the wave functions. The resulting quasi-two-dimensional densities of states give the WSL its characteristically strong absorption near the band edge. Care is taken to not fully localize the wave functions, however, since an electron miniband is required to allow vertical transport of the photoexcited minority carriers.

The use of WSLs in photodiodes was first reported by Fuchs *et al.*,[3] who investigated structures designed for MWIR laser operation. Mixed results were obtained relative to photodiodes employing binary and ternary type-II superlattices (BSLs and TSLs), with the WSLs exhibiting good transport characteristics, but quantum efficiency (QE) hampered by large series resistance. We have more recently resumed the investigation of WSL photodiodes, extending operation to the LWIR and VLWIR bands.[4] Initial designs adapted from WSL lasers yielded transport results comparable to those for BSL and TSL photodiodes, but significantly lower QEs. Since transmission measurements confirmed strong absorption, this was attributed to poor collection of the photoexcited carriers. It also raised concerns that WSLs, with their longer period, additional interfaces, high Al content, and reduced electron mobility, might necessarily have low QE.

In this letter we describe a second generation of WSL-based LWIR photodiodes, in which improvements to the design and material quality have strongly reduced minority-carrier losses and substantially improved the QE. By measuring QE in a series of WSL *p-i-n* photodiodes grown with identical heterostructures but with varying background-doped *i*-region (BD-region) thickness, we are able to extract the minority-carrier diffusion length.

Figure 1 specifies the thickness and composition of each layer employed in the four-constituent periodic WSL structure, which was designed for a nominal band gap of 11.3 μm. Here the AlSb barriers of the earlier WSL photodiodes are replaced by quaternary barrier layers (QBLs), consisting of $Al_{0.4}Ga_{0.49}In_{0.11}Sb$. Since the QBL contains 60% less Al, its optimal growth temperature is much closer to that of the InAs and InGaSb layers. The QBL conduction band offset with respect to InAs is also substantially reduced, from 2.1 eV for AlSb barriers to 1.3 eV for the QBL. This results in a near doubling of the electron miniband width, from 20 to 35 meV, and therefore an enhancement of the vertical electron mobility.

Five WSL *p-i-n* photodiodes were grown with BD regions having thicknesses of 1, 1.5, 2, 3, and 4 μm, in a Riber compact 21 T solid-source molecular beam epitaxy (MBE)

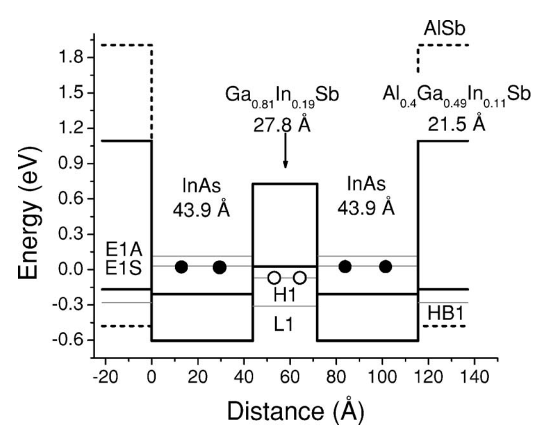


FIG. 1. Band profiles and energy levels at $k=0$ of enhanced WSL with quaternary barrier layers. Dashed lines indicate the position AlSb bands for comparison.

[a]Electronic mail: aifer@estd.nrl.navy.mil

 

system. Each *p-i-n* structure was grown on a *n*-type (Te doped $1\times10^{17}$ cm$^{-3}$) GaSb substrate, beginning with a thick $p^+$-GaSb contact layer doped with Be to $(1-3)\times10^{18}$ cm$^{-3}$, followed by a 0.1-$\mu$m-thick *p*-WSL that was Be doped to $4\times10^{17}$ cm$^{-3}$. The BD region was grown next, followed by 0.33 $\mu$m of $n^+$-WSL, Si doped to $4\times10^{17}$ cm$^{-3}$. The structures were capped with a 10-nm-thick $n^+$-InAs contact layer, Si doped to $4\times10^{17}$ cm$^{-3}$.

The target structure was designed to be strain compensated with neutral interfaces. This was motivated by an earlier study[5] that linked strong degradation of the photoluminescence (PL) intensity with the use of group III soaks to force InSb-like interface bonds. Even without group III soaks, however, cross-sectional scanning tunneling microscopy has revealed that MBE background levels and segregation can still induce the predominance of a particular bond type, and hence strain.[6] WSL test structures were therefore grown and evaluated for strain and periodicity by x-ray diffraction and for band gap and overall material quality by PL measurements. To the extent that background As levels and Sb segregation could be eliminated, the nominally lattice matched WSL alloy recipe was typically adjusted in the final calibration growth to minimize strain. While this procedure produced wafers with negligible strain (120 ppm maximum, $<50$ ppm typical) and uniformly high PL intensity, superlattice period was allowed to vary by as much as 5% (2 ML), resulting in a cutoff wavelength range from 9.3 to 11.3 $\mu$m. This was acceptable for the purposes of this study since peak QE is fairly insensitive to band gap.

Unpassivated, circular mesa diodes with 100–400 $\mu$m diameters were isolated by wet etching to a depth of 1.5–4.5 $\mu$m to the $p^+$-GaSb contact layer. Ti/Pt/Au Ohmic contacts were then deposited on both the $n^+$-InAs top and exposed $p^+$-GaSb bottom contact layers. The contacts were windowed or were small relative to the mesa size to provide optical access to the top-illuminated photodiodes.

The external QE was determined from the photocurrent excited in the sample by a calibrated blackbody operating at 1000 K and at a distance of 10.9 in. The blackbody flux, chopped at 37 Hz, was incident through a narrow bandpass filter, centered at 5.34 $\mu$m with a 0.35 $\mu$m full width at half maximum. To reduce stray reflections, the sample was enclosed in a cold shield with a half-angle field of view of $\approx 10°$. The average QE within the filter passband was then used to rescale the normalized QE spectrum obtained with a Fourier transform infrared spectrometer. Independent QE measurements on several samples were also performed at Rockwell Scientific Co. and Northwestern University.

In Fig. 2, typical QE spectra for each *p-i-n* photodiode are plotted for comparison. The QE is seen to increase systematically with absorber thickness, with the external QE (measured at 8.6 $\mu$m and averaged over 20 photodiodes) reaching a value of 34% for the 4-$\mu$m-thick device, which had a 50% power responsivity cutoff wavelength of 11.3 $\mu$m. This is among the highest reported for an antimonide type-II superlattice photodiode.[7,8] The *I-V* characteristics yielded average dynamic-impedance-area products ($R_0A$) of 10–20 $\Omega$ cm$^2$ at 80 K, also comparable to the best type-II values,[9] although still about a factor of 10 lower than the state of the art for HgCdTe photodiodes in this wavelength range. Surface resistivities of $\approx(1-2)\times10^4$ $\Omega$ cm along the unpassivated sidewalls were obtained from the inverses of the slopes of $(R_0A)^{-1}$ versus mesa perimeter-to-area

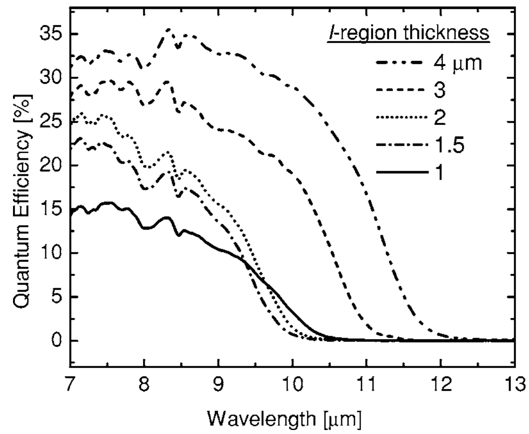


FIG. 2. Quantum efficiency spectra of WSL photodiodes with 1–4-$\mu$m-thick background-doped *i*-regions. Each spectrum is representative of the average for the sample.

ratio. These relatively high values of surface resistivity indicate suppressed rates of band-to-band and trap-assisted tunneling, which are prevalent where the high field region of the junction is exposed. We believe that the suppression of tunneling current in WSLs is due mainly to the very large electron effective mass along the growth axis, relative to that of binary and ternary type-II superlattices.

In a *p-i-n* photodiode, the quantum efficiency is largely determined by three factors: the absorption coefficient, the background impurity concentration in the BD region ($N_{\text{bgnd}}$), and the minority-carrier diffusion length ($L_n$). While the absorption coefficient determines the rate of optical generation, $N_{\text{bgnd}}$ and $L_n$ determine the volume over which photoexcited carriers can contribute significant photocurrent, through drift or diffusion processes, respectively. In an ideal *p-i-n* diode, the background impurity concentration is negligible and the built-in electric field extends across the entire *i* region and sweeps all photoexcited carriers across the junction. If the residual doping levels are appreciable, however, the field is restricted to a relatively short depletion region and most photoexcited carriers must diffuse a significant distance across the quasineutral *i* region to be collected. In this case, the minority-carrier diffusion length is a critical factor determining the detector quantum efficiency.

This behavior can be quantified using Hovel's expression[10] for the external QE of a *p-n* junction, with the surface recombination velocity set equal to zero. The total QE is expressed as sum over three regions,

$$\text{QE} = \text{QE}_{p\text{-}n} + \text{QE}_{\text{SCR}} + \text{QE}_{n\text{-}p}. \quad (1)$$

The contribution from the space charge region (SCR) is

$$\text{QE}_{\text{SCR}} = (1-R)(e^{-\alpha x_n} - e^{-\alpha x_p}), \quad (2)$$

where QE depends only on the reflectivity of the top surface $R$, on the absorption coefficient $\alpha$, and on $N_{\text{bgnd}}$ through the boundaries of the $n$ and $p$ depletion regions $x_n$ and $x_p$. The collection of minority electrons from the quasineutral $p$ region ($\text{QE}_{n\text{-}p}$), however, is a strong function of the electron diffusion length $L_n$ and its ratio with the width of this region $W_H$,

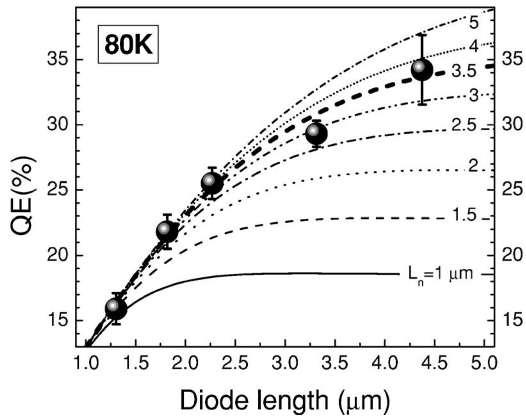


FIG. 3. Scatter plot of peak QE of WSL photodiodes vs length, from the beginning of the *n* region to the end of *p*-background-doped region. Lines are plots of Hovel's expression [Eqs. (1)–(3)], with the electron diffusion length as a fitting parameter.

$$\mathrm{QE}_{n\text{-}p} = (1-R)\frac{\alpha L_n}{(\alpha L_n)^2 - 1} e^{-\alpha x_p}\left[\alpha L_n - \frac{\sinh(W_H/L_n) + \alpha L_n e^{-\alpha W_H}}{\cosh(W_H/L_n)}\right]. \quad (3)$$

A similar contribution from the quasineutral $n$ region, $\mathrm{QE}_{p\text{-}n}$, is minimal because that layer is thin and heavily doped and has a low minority-carrier hole mobility.

The background doping of the $i$ region was determined from measurements on a Hall sample, consisting of a 2-$\mu$m-thick undoped WSL grown over a 1-$\mu$m-thick lattice matched $\mathrm{AlAs}_{0.4}\mathrm{Sb}_{0.92}$ layer to isolate the WSL from the conductive $n$-GaSb substrate. A quantitative mobility spectrum analysis[11] of the magnetic-field-dependent (0–9 T) Hall data determined electron and hole carrier densities and mobilities versus temperature. The results show a $p$-type background concentration of $\approx 2\times10^{15}\ \mathrm{cm}^{-3}$ with a mobility of $\approx 5000\ \mathrm{cm}^2/\mathrm{V\,s}$ at 80 K.

One remaining issue is that the line shapes exhibited in Fig. 2 are atypical of the WSL spectra expected from the absorption measurements, since they lack the characteristic peak near cutoff, and also exhibit sharp, oscillatory features having a fixed pattern. These features correspond to the transmission spectrum of the metal-filled epoxy used to bond the samples to the gold plated chip carriers. Transmission measurements show that the 500-$\mu$m-thick $n$-GaSb substrates (Te doped $1\times10^{17}\ \mathrm{cm}^{-3}$) transmit nearly 85% of the incident light not reflected at the interface (at 7.5 $\mu$m). It is therefore evident that multiple internal reflections contribute significantly to the measured QE. Based on QE measurements of a $p$-$i$-$n$ photodiode using the same heterostructure with a 2-$\mu$m-thick BD region grown on an absorbing $p$-GaSb substrate, we estimate that the measured QE is enhanced by 35% for the 4-$\mu$m-thick BD-region sample to 55% for the sample with the 1-$\mu$m-thick absorber. The corresponding single-pass QE values are then 10%, 14.6%, 17.5%, 20%, and 25% for the 1-, 1.5-, 2-, 3-, and 4-$\mu$m-thick absorber layer samples, respectively. This effect results in a further underestimation of the diffusion length, since the relative increase in QE due to reflections increases as the strongly absorbing BD-region thickness decreases.

In Fig. 3, solid circles are used to plot the measured QE peak nearest cutoff as a function of diode length including the $n$-doped and BD regions. Simulations using Hovel's expression (lines), with the electron diffusion length as a fitting parameter, are plotted for comparison. The best fit is obtained for an electron diffusion length of $L_n \approx 3.5\ \mu$m and an absorption coefficient of $2200\ \mathrm{cm}^{-1}$ at 7.5 $\mu$m, which represents a lower bound on $L_n$ since we set the surface recombination velocity to zero. While transmission measurements on the photodiode wafers yielded a value of $1600\ \mathrm{cm}^{-1}$ for the absorption coefficient, the value used for fitting is enhanced by 40% owing to multiple reflections in packaged devices as discussed above. Finally, almost no enhancement in photoresponse under reverse bias was observed in photodiodes with active regions less than 4 $\mu$m thick, in further confirmation that the diffusion length was in excess of 3 $\mu$m.

Our results demonstrate that despite the WSL's additional complexity, including twice as many interfaces per period and reduced electron mobility along the growth axis, WSL photodiodes can achieve high QE relative to other type-II superlattice systems.

The authors gratefully acknowledge Manijeh Razeghi and Andrew Hood at Northwestern University and Gernot Hildebrandt at Rockwell Scientific Co. for providing independent QE measurements of several of the samples in this letter. This work was supported by the Office of Naval Research and the Missile Defense Agency.

[1]J. R. Meyer, C. A. Hoffman, F. J. Bartoli, and L. R. Ram-Mohan, Appl. Phys. Lett. **67**, 757 (1995).
[2]C. L. Canedy, W. W. Bewley, J. R. Lindle, I. Vurgaftman, C. S. Kim, M. Kim, and J. R. Meyer, Appl. Phys. Lett. **86**, 211105 (2005).
[3]F. Fuchs, L. Burkle, R. Hamid, N. Herres, W. Pletschen, R. E. Sah, R. Kiefer, and J. Schmitz, Proc. SPIE **4288**, 171 (2001).
[4]E. H. Aifer, J. G. Tischler, J. H. Warner, I. Vurgaftman, J. C. Kim, J. R. Meyer, B. R. Bennett, L. W. Whitman, E. M. Jackson, and J. R. Lorentzen, Proc. SPIE **5732**, 259 (2005).
[5]C. L. Canedy, W. W. Bewley, C. S. Kim, M. Kim, I. Vurgaftman, and J. R. Meyer, J. Appl. Phys. **94**, 1347 (2003).
[6]E. M. Jackson, G. Boishin, E. H. Aifer, B. R. Bennett, and L. W. Whitman, J. Cryst. Growth **270**, 301 (2004).
[7]Y. Wei, A. Gin, and M. Razeghi, Appl. Phys. Lett. **80**, 3262 (2002).
[8]Y. Wei, A. Hood, V. Yazdanpanah, M. Razeghi, M. Z. Tidrow, and V. Nathan, Appl. Phys. Lett. **86**, 091109 (2005).
[9]R. Rehm, M. Walther, F. Fuchs, J. Schmitz, and J. Fleissner, Appl. Phys. Lett. **86**, 173501 (2005).
[10]H. J. Hovel, *Semiconductors and Semimetals* (Academic, New York, 1975), Vol. 11, pp. 17–20.
[11]I. Vurgaftman, J. R. Meyer, C. A. Hoffman, D. Redfern, J. Antoszewski, and L. Faraone, J. Appl. Phys. **84**, 4966 (1998).